Searches for point-like neutrino sources with the ANTARES neutrino telescope

J. Barrios-Martí[1] *on behalf of the ANTARES collaboration*

[1]Instituto de Física Corpuscular (CSIC-Universitat de València) c/ Catedrático José Beltrán, 2 E-46980 Paterna, Valencia, Spain

DOI: http://dx.doi.org/10.3204/DESY-PROC-2016-05/26

ANTARES is the largest undersea neutrino telescope currently in operation. This telescope has been taking data continuously since 2007 with the aim to detect neutrinos from astrophysical sources. A review of the point-like neutrino sources with the ANTARES telescope is presented. The latest results of the all-flavour neutrino point-source analysis with data from 2007 to 2013 and the results of the first combined ANTARES and IceCube analysis are described.

1 The ANTARES neutrino telescope

ANTARES is the first undersea neutrino telescope [1]. It is in continuous operation since 2006, and completed since 2008. It is located in the depth of the Mediterranean Sea (2475 m deep) at coordinates (42° 48' N, 6° 10' E), 40 km South of Toulon (France). It consists of 12 lines of 350 m height with inter-line separations between 60 to 75 m, which house a total of 885 Optical Modules (OMs). An OM consists of a 10" photomultiplier tube (PMT) contained inside a 17" glass sphere. The OMs are facing downward at an angle of 45° in order to improve the detection of up-going muon-neutrinos. They are organized in triplets, so that there are 25 triplets (storeys) on each line, with a distance between consecutive storeys in the same line of 15m.

The detection principle is based on the indirect detection of high energy neutrinos which interact via charged current (CC) or neutral current (NC) interactions with a nucleus inside or nearby the detector volume. In case a muon neutrino interacts via CC, it produces a muon which can travel a long distance before decaying. Since this muon travels at relativistic speeds in water, Cherenkov radiation is emitted. This type of events are usually referred as *track-like*. A fraction of the photons emitted from this radiation are detected by the PMTs, which produces a signal or *hit*. With the collected charge and the time of arrival, a reconstruction of these events is performed. Tau neutrinos can also produce this type of events.

On the other hand, all neutrinos interacting via NC or electron neutrinos and sometimes tau neutrinos via CC can produce *cascade-like* events. In this case, a fraction of the original neutrino energy is deposited via a hadronic and/or an electromagnetic shower. The photons coming from these showers expand spherically from the interaction vertex. The reconstruction is performed with the detected photons coming from the shower.

2 ANTARES point-source search including cascades

For the first time, a search for point-like sources including cascades has been performed. The addition of cascades provides the ability to perform these searches with all flavours of neutrinos both via charged current and neutral current interactions.

2.1 cascade reconstruction

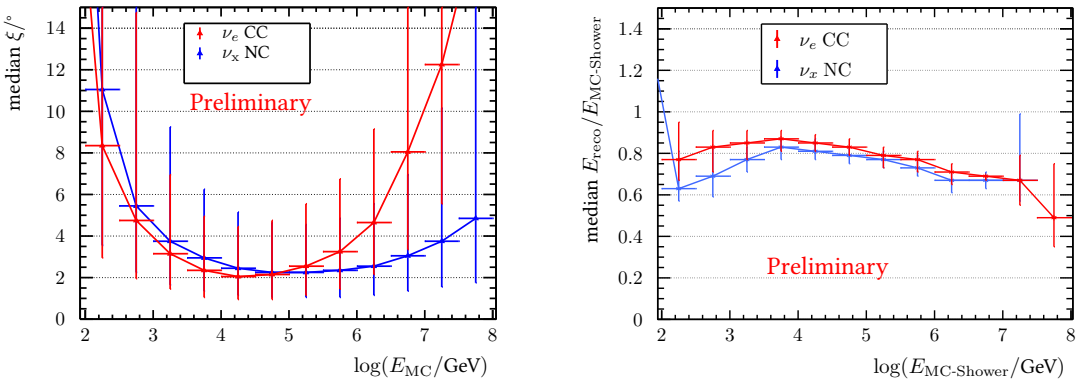

Figure 1: Left: Angular resolution for cascades coming from ν_e charged current interactions (red) and from NC interactions of neutrinos of all flavours (blue). Right: median energy resolution between the reconstructed energy and the deposited energy of the interaction. Both figures have been calculated for events with neutrino-interaction vertices of $|Z_{vertex}| < 200$ m, $\rho_{vertex} < 90$ m from the detector centre. The error-bars in the y axis denote the 1σ region.

A new reconstruction for cascade events [2] was developed to include these events in point-like source searches. This reconstruction is based on a two-step procedure.

The first step consists on the interaction vertex reconstruction, where an expanding spherically shell of photons from this point is assumed. This is done via a pre-fit with the information of all selected hits, in which we assume that they have been produced from the same interaction. That leads to a set of equations which are minimised via an M-estimator fit,

$$M_{Est} = \sum_{i}^{N} \left(q_i \sqrt{1 + t^2_{i-\mathrm{res}}/2} \right) \tag{1}$$

where q_i and $t_{i-\mathrm{res}}$ denote the charge and the time residual (difference between the expected and the actual arrival time) of the hit i.

The second step consists on the direction reconstruction. In this case, all hits coming from a triggered event in a time residual window of -200 $< t_{res} <$ 500 ns are considered, where the t_{res} is the time residual with respect to the previously fitted vertex. The direction of the cascade is then obtained by performing a maximisation of a likelihood, defined as:

$$L = \sum_{i=1}^{N_{\text{selected}}} \log\left[P_{q_i>0}(q_i|E_\nu, d_i, \phi_i, \alpha_i) + P_{bg}(q_i)\right] + \sum_{i}^{N_{PMTs\ without\ hits}} \log\left[P_{q=0}(E_\nu, d_i, \phi_i)\right]. \quad (2)$$

In this equation, $P_{q_i>0}$ denotes the probability for a PMT, i, to have measured a charge q_i, $P_{q=0}$ is the probability for an absence of a detection in a PMT, and P_{bg} is the probability for a hit to be originated via background. All of these probabilities depend on the charge of the hit, q_i. Also, $P_{q_i>0}$ and $P_{q=0}$ depend on the neutrino energy, E_ν, the distance between the PMT i and the vertex of the interaction, d_i, the angle between the neutrino direction and the vector which connects the PMT i and the vertex of the interaction, ϕ_i, and the angle between the direction of the PMT with the same vector, α_i.

The performance of this reconstruction can be seen in figure 1. A median angular resolution between 2° and 4° degrees can be achieved for contained events (events within $|Z_{vertex}| < 200$ m, $\rho_{vertex} < 90$ m from the detector center according to our simulations) with neutrino energies of E_ν between 10^3 and 10^6 GeV for electron neutrino events interacting via CC. An estimate of the angular resolution of the cascade reconstruction can be obtained by using a data sample dominated by atmospheric muons. These events can be reconstructed both as track-like events and as cascades. Figure 2 shows the angular difference between the directions obtained from these two reconstructions for a loose cut dominated by atmospheric muons. The low difference between the reconstructed directions of both reconstructions shows the performance of the cascade reconstruction.

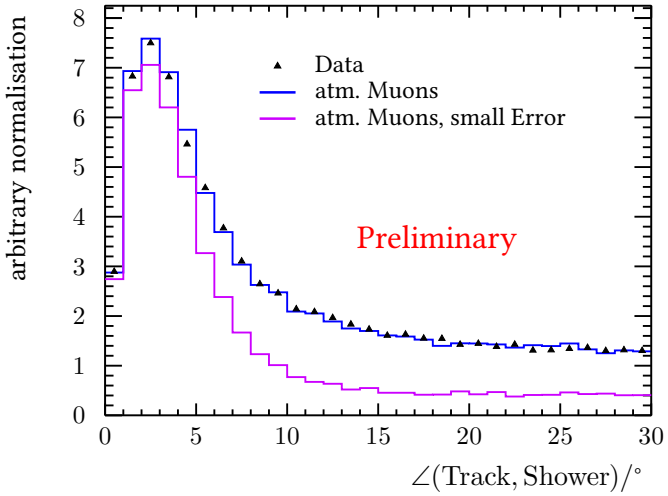

Figure 2: Angular difference between the reconstructed directions given by the track and cascade reconstructions. Black dots: Values obtained from data. Blue line: Values obtained from simulations. Magenta line: Values obtained for atmospheric muons from simulations with an angular resolution in the cascade channel lower than 5°.

2.2 Search method

The data sample contains data recorded from Jan 29, 2007 to Dec 31, 2013. The event selection for the track-like channel is identical to the last published point-source analysis [3], which consists on a cut on the reconstructed zenith angle, $cos(\theta_{track}) < 0.1$, an angular error estimate of $0 < \beta_{track} < 1°$, and a quality of the reconstructed track of $\Lambda_{track} >$ -5.2. These parameters are obtained from the track reconstruction mechanism, which uses a maximum likelihood (ML) method [4, 5]. This reconstruction is based on a multi-step procedure to fit the direction of the muon by maximising the Λ_{track} parameter. The angular error estimate, σ, is calculated from the uncertainty on the zenith and azimuth angles extracted from the covariance matrix.

The event selection for the cascade channel is obtained via a set of multiple cuts. First of all, a veto of the events which have been selected in the track channel is performed. Secondly, only events reconstructed as up-going or with almost horizontal directions ($\cos(\theta_{sho}) < 0.1$), and with a reconstructed interaction vertex close or inside the detector volume ($\rho_{show} < 300$m, $Z_{show} < 250$m) are included. Additionally, a maximum angular error estimate of 10° degrees is allowed. A combined cut on the GridFit Ratio [6] parameter and the number of selected hits by the cascade reconstruction is performed. Finally, a cut on a muon/cascade likelihood discrimination parameter and a cut on the ratio between the collected charge before and after the expected expected time recorded by the OMs is applied.

Afer this criteria, a total number of 6490 track-like and 172 cascade-like neutrino candidates are obtained. Figure 3 shows the location of these events in equatorial coordinates.

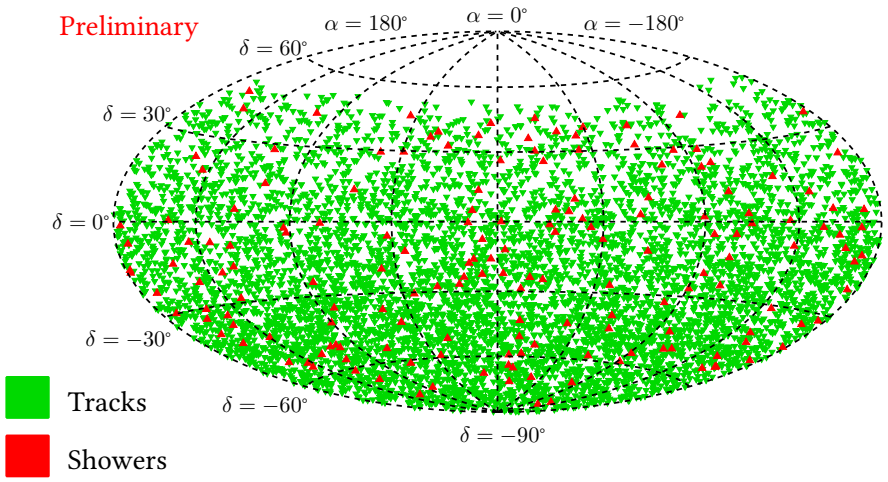

Figure 3: Skymap in equatorial coordinates of the reconstructed directions of the track-like (green) and cascade-like (red) events.

An unbinned likelihood maximisation with an extended likelihood definition is performed in order to search for excesses of events. This likelihood takes into account the directional information and the reconstructed number of hits, $\mathcal{N}$ as information of each event. The likelihood, as a function of the total number of fitted signal events, μ_{sig}, can be expressed as:

$$\log L_{\mathrm{s+b}} = \sum_{\mathcal{S}} \sum_{i \in \mathcal{S}} \log \left[\mu^{\mathcal{S}}_{\mathrm{sig}} \cdot PSF^{\mathcal{S}}(\Delta\Psi_i) \cdot N^{\mathcal{S}}_{\mathrm{sig}}(\mathcal{N}_{\mathrm{i}}) + B^{\mathcal{S}}(\delta_i) \cdot N^{\mathcal{S}}_{\mathrm{bkg}}(\mathcal{N}_{\mathrm{i}}) \right] - \mu^{\mathcal{S}}_{\mathrm{sig}} + P(\mu^{\mathrm{sh}}_{\mathrm{sig}} | \mu^{\mathrm{tr}}_{\mathrm{sig}} \cdot \mathcal{A}^{\mathrm{sh}}(\delta_{\mathrm{s}}) / \mathcal{A}^{\mathrm{tr}}(\delta_{\mathrm{s}})). \quad (3)$$

where S denotes the track (tr) or cascade (sh) sample, $\mathrm{PSF}(\Delta\Psi_i)$ is the point spread function value for a given event i at a distance $\Delta\Psi_i$ from the assumed source, $B(\delta)$ is the background rate of data events as a function of the declination δ, $N^{\mathcal{S}}_{\mathrm{sig}}(\mathcal{N})$ and $N^{\mathcal{S}}_{\mathrm{sig}}(\mathcal{N})$ are the probability density functions which give the probability for an event to be signal or background given the number of hits $\mathcal{N}$, and $\mathcal{A}^S(\delta_s)$ is the acceptance (proportionality constant between a flux normalisation, Φ_0 and the number of expected events detected given an E^{-2} source spectrum at a declination δ_s). The poissonian term, $P(\mu^{\mathrm{sh}}_{\mathrm{sig}} | \mu^{\mathrm{tr}}_{\mathrm{sig}} \cdot \mathcal{A}^{\mathrm{sh}}(\delta_{\mathrm{s}}) / \mathcal{A}^{\mathrm{tr}}(\delta_{\mathrm{s}}))$ is included to take into account the expected ratio between the number of signal events between the track and cascade channels. Figure 4 shows the acceptance for the cascade and track channels.

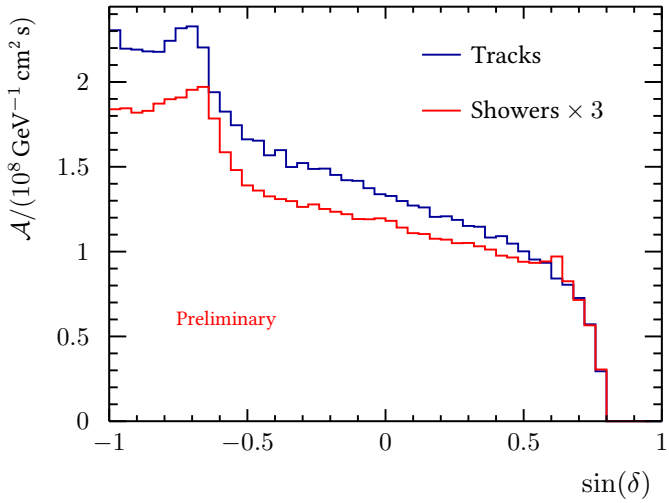

Figure 4: Acceptance for the track (blue) and cascade (red) channel assuming an E^{-2} spectrum. The cascade acceptance has been multiplied by 3 in this figure.

From this likelihood, a test statistic, TS, is defined so that $TS = \log L_{\mathrm{s+b}} - \log L_{\mathrm{b}}$, where L_{s+b} is the maximised likelihood, and L_b is the likelihood value for the background only case.

Different search strategies are followed in order to look for candidate clusters which could exceed the expected background. In the full sky search, the whole sky is scanned. Per each cluster, also the direction of the hypothetical source is fitted. In the candidate list search, the location of 52 known high-energy gamma-ray emitters are considered, where the coordinates of the source are fixed. A separate candidate list search for the location of the eight track-like events from the Southern Sky observed by the IceCube experiment in their 3 year High Energy neutrino sample [7] is considered, where the fitted location of the fitted source is set to twice the angular error estimate of the IceCube events. Finally, a scan over the region around the galactic center (half-axis radii of 30° in galactic longitude, and 15° degrees in latitude) is performed.

2.3 Results

No significant clusters of events are observed in this analysis. The most significant cluster in the full sky search is found at a location of (α, δ) = (–46.8°, –64.9°) in equatorial coordinates with a post-trial significance of 4.2% (2.0σ in the two-sided convention). A total of 17(7) track-like events are observed within 3(1)° degrees and 1 cascade event within 10°. The most significant cluster of the candidate list search corresponds to the one corresponding to the location of HESSJ0632+057, with a post-trial significance of 20% (1.27σ). A total of 6(1) track events are observed within 3(1)°, and a total of 3 cascades are observed within 15°. The most signal-like cluster corresponding with the location of an IC event corresponds to (α, δ) = (130.7°, 29.5°), associated with IC track ID3. Finally, the most significant cluster of the search around the Galactic Centre is observed at (α, δ) = (110.0°, 50.8°) with a post-trial significance of 74% (0.33σ).

Limits from the 52 candidate sources and the sensitivity at a 90% confidence level for a fixed-source search with an E^{-2} energy spectrum are reported in figure 5, which present the best sensitivities for a large fraction of the Southern sky. The comparison with the 4 year analysis of IceCube is also presented.

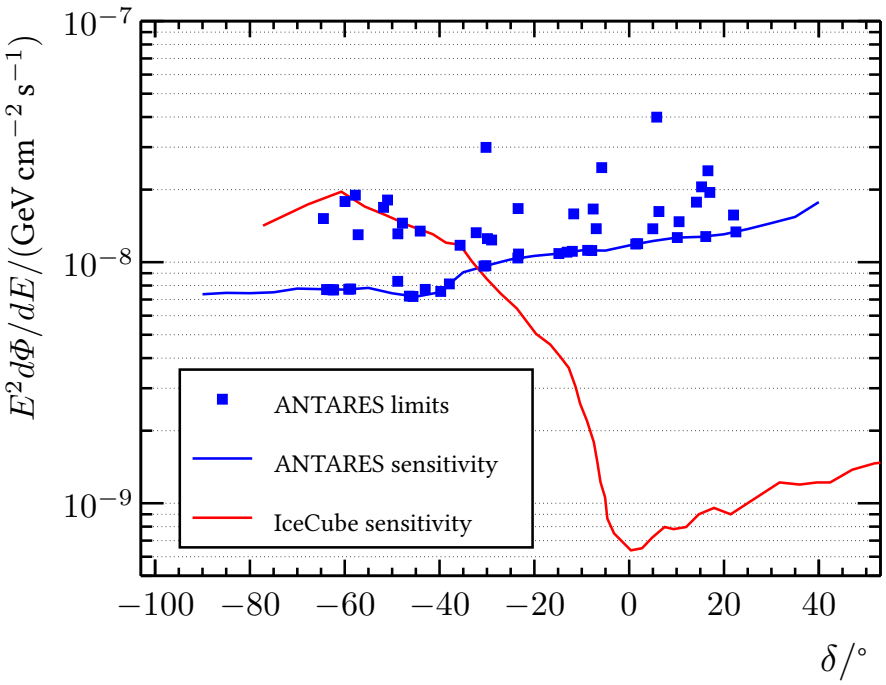

Figure 5: 90%CL limits and sensitivities following the Neyman approach [8]. The blue dots correspond to the limits of the 52 candidate sources. The blue line denotes the sensitivity for a point-source using a fixed-source analysis in this analysis. As a comparison, the sensitivity for the 4 year point-source analysis from IceCube is present.

3 Combined ANTARES-IceCube point-source analysis

The results of a search for point-like sources with data collected from the ANTARES and IceCube experiments were published recently[9]. Despite the significantly smaller volume of ANTARES compared with IceCube, its location provides a view of the Southern sky with significantly reduced background for neutrino energies below 100 TeV. The complementarity of both detectors with respect to sources coming from the Southern sky is due to the different geographical location, size and atmospheric muon background, allowing for a gain in sensitivity by combining data from both detectors.

The data sample corresponds to all events coming from the Southern Sky included in the three-year IceCube point-source analysis [10] and the 2007-2012 ANTARES one [3]. No cascade-like events were included in this analysis. The ANTARES sample contains data recorded from Jan 29, 2007 to Dec 31, 2012, whereas the IceCube one corresponds to data collected from Apr 5, 2008 to May 13, 2011 with the partially completed detector, and without the use of the Deep Core strings.

No significant clusters were found in this search. Figure 6 shows the sensitivities and limits obtained for the cases of an E^{-2} and a $E^{-2.5}$ energy source spectra. They are compared with the individual samples used in this analysis. The region of improvement due to the combination of the samples varies with the assumed energy spectrum of the source. An improvement factor of about 2 can be reached for an E^{-2} spectrum in regions close to the Galactic Centre. For steeper energy spectra the area of the sky with an improved sensitivity switches to declinations closer to the equator.

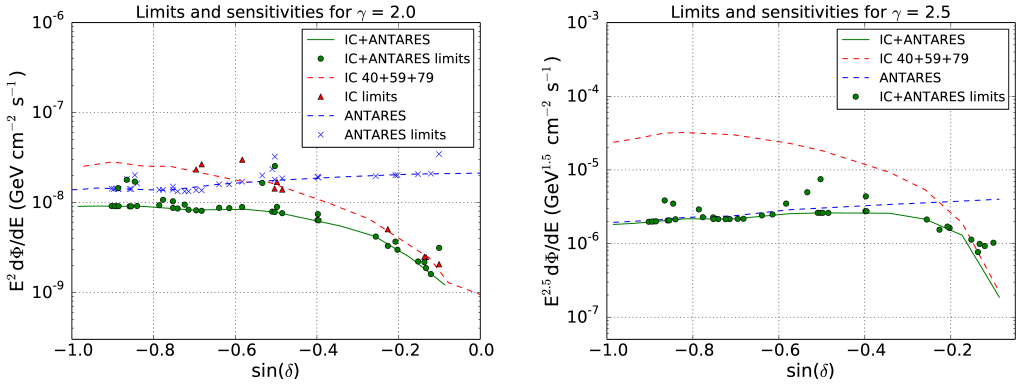

Figure 6: Point source sensitivities and limits for a 90% CL using the Neyman method [8] for energy spectra of E^{-2} (left) and $E^{-2.5}$ (right). The green line indicates the sensitivity for the combined search. Red and blue curves indicate the sensitivities for the individual IceCube and ANTARES analyses, respectively. As reference, the declination of the Galactic Center is approximately at $\sin(\delta = -29°) \approx$ -0.48.

4 Conclusions

A review of the latest results of point-like neutrino source searches with the ANTARES neutrino telescope has been shown. The first search for point-sources using both cascade and track events has been presented, with no statistically significant signal clusters found. A specific reconstruction for cascades had to be developed, leading to median angular resolutions between 2 and 4° for energies between 10^3 and 10^6 GeV. 90% CL limits and sensitivities for this search have been presented. A brief summary of the first combined analysis using data both from the ANTARES and IceCube experiments is also given, where an improvement up to a factor of 2 in sensitivity is achieved.

Acknowledgments

We gratefully acknowledge the financial support of Plan Estatal de Investigación (refs. FPA2015-65150-C3-1-P, -2-P and -3-P, (MINECO/FEDER)), Severo Ochoa Centre of Excellence and MultiDark Consolider (MINECO), Prometeo and Grisolía programs (Generalitat Valenciana), Spain., and Atracció de Talent of Universitat de València, Spain.

References

[1] M. Agueron et al. (ANTARES Collaboration), Nucl. Instrum. Meth., **A656**, 11, (2011).

[2] T. Michael, Light at the end of the Shower, PhD Thesis, NIKHEF, Amsterdam (2016).

[3] S. Adrián-Martínez et al. (ANTARES Collaboration) ApJ, **786**, L5 (2014).

[4] S. Adrian-Martinez et al. (ANTARES Collaboration) ApJ, **760**, 53 (2012).

[5] S. Adrian-Martinez et al. (ANTARES Collaboration) JCAP, **1303**, 006 (2013).

[6] E. L. Visser, Neutrinos from the Milky Way, PhD Thesis, NIKHEF, Amsterdam (2015).

[7] M. G. Aartsen et al. (IceCube Collaboration), Phys. Rev. Lett. **113**, 101101 (2014).

[8] Neyman J. Phil. Trans. Royal Soc. London A, **236**, 333 (1937).

[9] Adrian-Martinez, S. et al. (ANTARES and IceCube Collaborations), ApJ. **823**, 65 (2016).

[10] Aartsen M. G. et al. (IceCube Collaboration), ApJ, **779**, 132 (2013).